Optical and in situ characterization of plasma oxidized Al for magnetic tunnel junctions

Document Version:

Publisher's PDF, also known as Version of Record (includes final page, issue and volume numbers)

Please check the document version of this publication:

• A submitted manuscript is the version of the article upon submission and before peer-review. There can be important differences between the submitted version and the official published version of record. People interested in the research are advised to contact the author for the final version of the publication, or visit the DOI to the publisher's website.

• The final author version and the galley proof are versions of the publication after peer review.

• The final published version features the final layout of the paper including the volume, issue and page numbers.

Link to publication

Optical and *in situ* characterization of plasma oxidized Al for magnetic tunnel junctions

P. LeClair,[a] J. T. Kohlhepp, A. A. Smits, H. J. M. Swagten, B. Koopmans, and W. J. M. de Jonge

Department of Applied Physics and COBRA, Eindhoven University of Technology, P.O. Box 513, 5600 MB Eindhoven, The Netherlands

An optical polarization modulation technique was adapted to provide a simple, fast, and flexible method for studying the kinetics and growth characteristics of thin oxide layers, using Al_2O_3 as an example. The optical technique allows precise determination of the amount of remaining metallic Al as a function of the initial Al thickness, while scanning a laser spot across the wedge. Optical data suggest that the oxide growth rate for the ultrathin layers may be dependent on the specific microstructure. *In situ* x-ray photoelectron spectroscopy performed on homogenous samples confirmed the interpretation of the optical results. © *2000 American Institute of Physics.* [S0021-8979(00)43208-1]

For fabricating reliable, high TMR (tunnel magnetoresistance) tunnel junctions,[1,2] optimization of the plasma oxidation process to ensure minimal unoxidized Al, while preventing oxidation of the underlying electrode, is of critical importance. However, few methods exist[2–5] for characterizing the growth of ultrathin oxidic layers. An optical polarization modulation technique was adapted to provide a simple, fast, and flexible method for studying the growth characteristics of thin oxide layers, with the potential for *in situ* process monitoring. Due to the large difference between the dielectric constant of Al ($\epsilon \approx -50 + 20i$ at $\lambda \approx 600$ nm) and its oxide ($\epsilon \approx 3.3$ at $\lambda \approx 600$ nm),[6] the Al–Al_2O_3 system provides an almost ideal case for optical analysis. Combined with the use of wedge-shaped Al structures and spatially resolved optical probing, submonolayer amounts of Al may easily be observed. In addition to the optical technique, *in situ* x-ray photoelectron spectroscopy (XPS) and scanning tunneling microscopy (STM) were performed, confirming the interpretation given by the optical technique, as well as to provide further information.

The oxidation experiments were performed both as a function of oxidation time (for fixed Al thickness) and as a function of Al thickness (for fixed oxidation times). XPS was utilized for these experiments in light of its extreme sensitivity (<1 ML[7]) and ability to provide chemical information, as well as the possibility to perform *in situ* studies on clean samples. However, XPS requires many individual samples, is time consuming, and has little potential for process monitoring. To this end, the optical polarization modulation technique was developed, which we describe presently. Using wedge shaped oxidized Al samples (3–4 Å/mm), a He–Ne laser ($\lambda = 632.8$ nm) polarized perpendicular to the plane of incidence (*s* polarized) was focused to a spot of approximately 100 μm and scanned across the wedge to allow probing as a function of Al thickness. The polarization of the light was modulated between right- and left-circularly polar-

ized light at a frequency f of 50 kHz using a photo-elastic modulator. After passing through a polarizer (analyzer), intensities at 50 kHz ($1f$) and at 100 kHz ($2f$) were monitored as a function of position on the wedge. To obtain an absolute calibration of the change in the $1f$ and $2f$ signals as a function of polarization rotation, the output of the signals were measured after rotating the analyzer by a known angle.

To investigate the oxidation process as a function of oxidation time, homogeneous ultrahigh vacuum magnetron sputtered samples of Si(111)/Ta 50 Å/Co 50 Å/Al d_{Al} were prepared and plasma oxidized for various times from 0–600 s in 0.1 mbar O_2. In order to judge the amount of ''instantaneous'' oxidation, samples were also exposed to 0.1 mbar for 10 s *without* plasma. The oxidation was performed in an incremental manner (i.e., a 20 s sample has been twice oxidized 10 s) to study the time evolution of the oxidation unambiguously. In addition, reference samples of Co, Al, CoO_x, and AlO_x were prepared, with the oxides prepared by 600 s plasma oxidation of thick metal layers. *In situ* STM on Si/Ta/Co/Al samples indicated flat films with small grains and a mean roughness of <3 Å for all layers. XPS intensities of the Al $2s$, Al $2p$, and Co $2p$ photoelectron lines were recorded with Mg K_α radiation, while the O $1s$ photoelectron line was recorded with Al K_α radiation. Figure 1(a) shows the Al $2s$ and $2p$ spectra for samples with differing oxidation times, all for a nominal Al thickness of 22 Å. For the unoxidized sample, no peak at the oxidic binding energy is observed,[7,8] while for only 10 s oxidation *without* plasma, significant Al oxide is clearly visible for both the $2s$ and $2p$ lines. With increasing oxidation time, the metallic Al XPS intensity monotonically decreases, while the oxidic Al XPS intensity monotonically increases. For 200 s oxidation, little metallic Al remains, and none is observable (≤ 1 ML) for 600 s.

Figure 1(b) shows the calculated O:(oxidized) Al ratio as a function of oxidation time, as obtained from the primary zero-loss intensities[7,8] of the oxidic Al $2p$ and O $1s$ peaks, using a 600 s oxidized Al sample (where no metallic Al could be detected) of the same thickness as a reference. It is

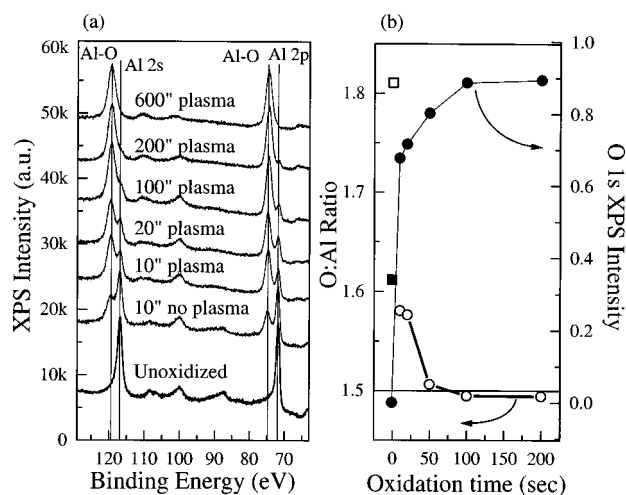[a] Author to whom correspondence should be addressed; electronic mail: pleclair@phys.tue.nl

FIG. 1. (a) Al 2*s* and 2*p* XPS spectra for various oxidation times. (b) O:Al ratio determined from Al 2*p* and O 1*s* lines (open) and O 1*s* intensity (closed), as a function of oxidation time. Unconnected points (squares) are for 10 s O$_2$ exposure *without* plasma. Nominal Al thickness for all samples was 22 Å.
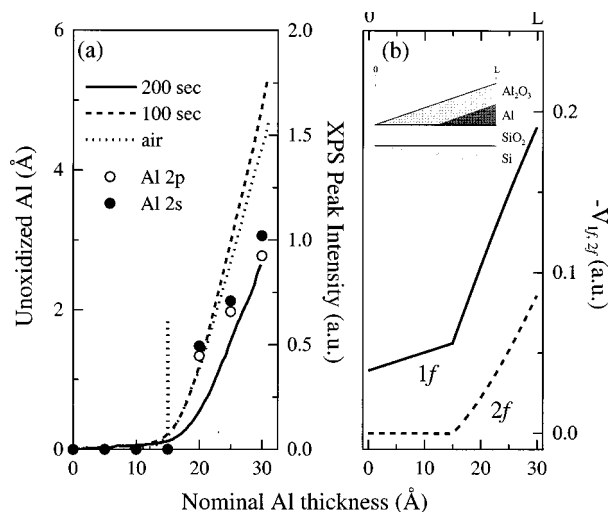

FIG. 2. (a) XPS peak intensities for Al 2*p* (open) and Al 2*s* (closed) as a function of nominal Al thickness for 200 s oxidized samples. Lines represent optical measurements on wedge samples for 100 (dashed) and 200 s (solid) plasma oxidation, and air (dotted) oxidation. Vertical line indicates the *maximal* thickness for which CoO was observed. (b) Calculated 1*f* (solid line) and 2*f* (dashed line) signals as a function of position on the wedge (see inset).

evident that the 10 s exposure to O$_2$ without plasma forms a significant amount of AlO$_x$, with a further steep decrease of the O:Al ratio in the first 10–20 s of plasma oxidation. By 100 s, the AlO$_x$ is nearly stoichiometric, also evidenced by Fig. 1(a), which shows only a small amount of metallic Al remaining. The O 1*s* XPS intensity is also plotted in Fig. 1(b), which exhibits an initial, rapid increase and becomes roughly constant beyond 100 s, in corroboration with the spectra and the O:Al ratio.

For experiments as a function of Al thickness, homogeneous samples of Si(111)/Ta 50 Å/Co 50 Å/Al d_{Al} were prepared as previously, while for the optical experiments, 0–30 Å wedge shaped samples of 3–4 Å/mm were grown on Si(111) or oxidized Si(111). Both types of samples were plasma oxidized in 0.1 mbar O$_2$ for 100 or 200 s, with several wedge samples air oxidized for several hours. Figure 2(a) shows the measured amount of unoxidized (''leftover'') Al as a function of the deposited Al layer thickness as measured by XPS (circles) with the Al 2*s* (closed) or 2*p* (open) line. The XPS data show no metallic Al for thicknesses below 15 Å, with a continuously increasing amount of metallic Al observed beyond ~15 Å.[9]

Figure 2(a) also shows the measured amount of unoxidized Al obtained from the optical measurements on oxidized Al wedges (lines). In order to determine the amount of remaining metallic Al from the optical measurements, model calculations were used to estimate the magnitude and dependencies of the 1*f* and 2*f* signals. These calculations were based on an idealized sample consisting of a linear Al wedge of 0 to 30 Å, which is homogeneously oxidized from the top [see Fig. 2(b)]. The two layers are placed on a Si substrate with a 20 Å SiO$_2$ native oxide layer [inset to Fig. 2(b)]. The reflection coefficients of *s*- and *p*-polarized light at the top interface of the stack are obtained by solving the Maxwell equations in each layer and matching the $\vec{E}$ and $\vec{B}$ vectors at each interface. The 1*f* and 2*f* signals can then be calculated using the Jones Formalism[9] for all optical components; the

result is shown in Fig. 2(b). From the simulation it is clear that the 2*f* signal is approximately linear with the Al thickness, while the 1*f* signal is proportional to both the Al and the Al$_2$O$_3$ thickness.

Returning to the optical data of Fig. 2(a), no measureable Al is visible for thicknesses below ~15 Å as with the XPS data. For all oxidation times, the amount of leftover metallic Al increases (approximately) linearly for thicknesses beyond ~15 Å also in agreement with the XPS data. The nominal thickness of leftover Al obtained from the model calculations is in rough agreement with the behavior of the XPS signals, and it can be seen that submonolayer amounts of metallic Al may be observed, confirming that this method may in principle be used to observe the oxidation process in ultrathin metallic layers. As expected, the 200 s oxidized sample shows less leftover Al than 100 s or air oxidized samples. Surprisingly, however, the onset of unoxidized Al occurs at approximately the *same* thickness for all samples.

The amount of Al$_2$O$_3$ was also determined by both methods. Figure 3(a) shows the intensity of the Al–O 2*s* (closed) and 2*p* (open) oxidic binding peaks determined by XPS. The amount of oxide increases with increasing Al thickness, showing a decreasing slope between 15–25 Å though it is not constant in this region. The amount of Al$_2$O$_3$ was also determined via the optical method, and although it showed some interesting features, they were found to depend sensitively on specific assumptions in the model (e.g., $\epsilon_{Al_2O_3}$, t_{SiO_2}, etc.). A detailed discussion of this data is therefore postponed to a future publication.

Figure 3(b) shows the Co 2*p* XPS spectra for samples of 23 Å Al and 5 Å Al after 200 s oxidation, as well as reference Co and CoO$_x$ spectra. For 23 Å Al, it is clear that only metallic Co is present, while for 5 Å, the Co oxidic satellite peaks are visible as well as a shift of the Co 2*p* lines, indicating oxidation of the underlying electrode. For all thick-
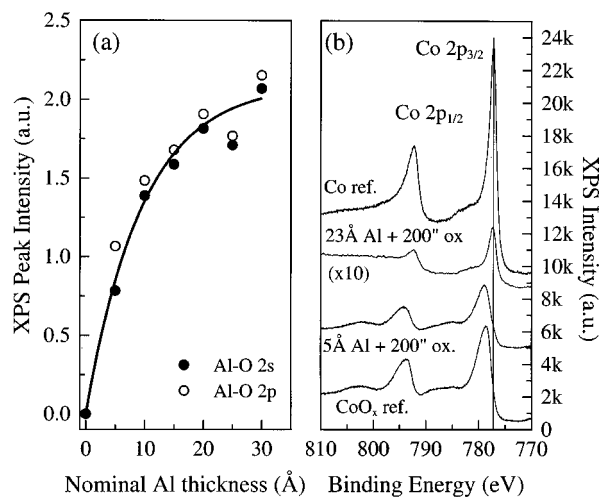
FIG. 3. (a) XPS peak intensities for Al–O $2p$ (open) and Al–O $2s$ (closed) as a function of nominal Al thickness for 200 s oxidized samples. The line is a guide to the eye. (b) Co $2p$ XPS spectra of 23 Å Al and 5 Å Al with 200 s oxidation, as well as reference Co and CoO$_x$ spectra.

nesses below $\sim$15–20 Å with 200 s oxidation, CoO was observed; the vertical line in Fig. 2(a) indicates the *maximal* thickness for which CoO was observed. This thickness is nearly the same thickness at which metallic Al began to be observed, indicating that disapperance of Co oxides and onset of leftover metallic Al are nearly coincident. The observation of Co oxides only after nearly all metallic Al is oxidized is not unexpected even in the presence of interface roughness, given the large difference in the free energy of formation for Al$_2$O$_3$ ($\Delta G_f^o = -378$ kcal/mol) and CoO ($\Delta G_f^o = -51.5$ kcal/mol) or Co$_3$O$_4$ ($\Delta G_f^o = -184$ kcal/mol).[6] The region of minimal CoO and metallic Al is the desired regime for formation of high TMR magnetic tunnel junctions.[1]

Returning now to the optical data of Fig. 2(a), the onset of leftover Al is nearly identical for 100 or 200 s oxidation, though the *slopes* of the curves show significant disparity between 100 and 200 s oxidized samples. This may indicate that the simple model of oxidation proceeding uniformly through the Al layer [see inset to Fig. 2(b)] may be too simplistic. Rather, it may be consistent with an initial, rapid oxidation via grain boundaries,[10] while longer times are needed to fully oxidize grain interiors. The unoxidized grain interiors would represent a relatively small volume fraction compared to the total amount of Al, and therefore, a small XPS or optical signal, but would require much longer times to fully oxidize. The thickness at which leftover Al is observed would then only differ in each case by the (small) amount of metallic Al remaining in the grain interiors. Further, the amount of metallic Al would also exhibit a smaller slope as a function of Al thickness for longer oxidation times, since the grain interiors are then more fully oxidized. More detailed microstructural data, as well as measurements for Al layers with differing microstructures, could clarify the mechanism(s) involved.

In summary, an optical polarization modulation technique was combined with *in situ* XPS to investigate the plasma oxidation of ultrathin Al layers. The optical technique allows precise determination of the amount of unoxidized Al with the use of wedge-shaped Al layers, confirmed by XPS measurements. The optical technique shows great potential for simple, flexible, and rapid optimization of oxidic tunnel barriers, and may be easily adapted for *in situ* use.

[1] J. S. Moodera, L. R. Kinder, T. M. Wong, and R. Meservey, Phys. Rev. Lett. **74**, 3273 (1995).
[2] J. S. Moodera, E. F. Gallagher, K. Robinson, and J. Nowak, Appl. Phys. Lett. **70**, 3050 (1997).
[3] M. Sharma, S. X. Wang, and J. H. Nickel, J. Appl. Phys. **85**, 7803 (1999).
[4] R. C. Sousa *et al.*, Appl. Phys. Lett. **73**, 3288 (1998).
[5] K. Knorr and J. D. Leslie, Solid State Commun. **12**, 615 (1973).
[6] J. A. Dean, *Lange's Handbook of Chemistry* (McGraw-Hill, New York, 1992).
[7] D. Briggs and J. C. Riviére, in *Practical Surface Science*, edited by D. Briggs and M. P. Seah (Wiley, New York, 1983).
[8] L. P. H. Jeurgens *et al.*, Appl. Surf. Sci. **144–145**, 11 (1999).
[9] P. Yeh, *Optical Waves in Layered Media* (Wiley, New York, 1988).
[10] L. G. Harrison, Trans. Faraday Soc. **57**, 1191 (1961).